

9. OPTICAL STATE-PREPARATION OF ATOMS

Jabez J. McClelland

Electron Physics Group
National Institute of Standards and Technology
Gaithersburg, Maryland

9.1 Introduction

In the study of a broad range of phenomena involving atoms, from collisions to spectroscopy to reaction dynamics, an increasing need has developed for probing ever deeper into the physical processes at work. The realization has evolved over the decades that to quantitatively study atomic interaction phenomena, it is necessary to experimentally resolve as many variables in the interaction as possible. For example, it is not enough to study the average thermal reaction rate of a collision-related process; instead, the process must be studied as a function of relative velocity and scattering angle. Eventually, it has become clear that the internal degrees of freedom of the atom play a crucial role, so these must be experimentally controlled as well. As a result of this need, the use of optical radiation, especially lasers, to control the internal states of atoms through optical pumping has become increasingly popular in atomic physics experiments.

The purpose of this chapter is to provide some guidelines for the experimentalist interested in performing a state-selected experiment using lasers. As this is meant to be a practical guide, an attempt is made to be fairly self-contained, quoting results from the literature as they are needed. Some knowledge is necessarily assumed, however, in particular regarding atomic structure and spectroscopic notation, and the fundamentals of the interaction between atoms and electromagnetic fields. In addition, some familiarity with the nature of quantum coherence will be useful.

Discussion in this chapter is limited to optical pumping in atomic beams, with a strong slant toward collision experiments. A complete review of optical pumping, as it is applied across atomic and molecular physics, would go far beyond the scope of this work. There is a large amount of literature relating to optical pumping in vapor cells, and also cooling and trapping of atoms, that there is simply not enough space to discuss. The reader should be aware of the crossovers with these other fields, though, because much can be learned from parallel developments. In particular, an excellent resource is the review article by Happer [1] on optical pumping in vapor cells.

As a result of the emphasis on collision work, this chapter focuses mostly on optical pumping process which selectively populate the magnetic sublevels of an atom. This is because of the great amount of interest that exists in probing the channels of a collision which are associated with alignment and orientation of the target. By controlling the magnetic sublevel populations of the target one can, in effect, control orientation and/or alignment, and hence conduct an experiment at the most fundamental level of state selection.

Much of the discussion here is devoted to rate equation calculations and their interpretation, rather than specific experimental arrangements. The reason for this is that the experimental arrangement for a typical optical pumping experiment is quite simple, consisting of an atom beam, a laser (often commercial), and some fluorescence detection. The crucial aspect of doing a good job in optical state-preparation lies in knowing the details of what is happening to the atoms as they interact with the laser. A good understanding of the processes involved and facility with modeling techniques are essential for this. The last section of this chapter is intended as a resource of relevant data on a number of specific atoms, in the hope that this will prove useful for the planning of experiments.

9.2 Basic Concepts

The two fundamental facts that make laser optical pumping possible are (a) when an atom is exposed to electromagnetic radiation at a frequency near resonance, transitions are induced between quantum states in the atom, and (b) if an atom is in an excited state, it will decay by spontaneous emission to a lower state. These phenomena lead to transfer of atomic population from one quantum state of the atom to another. By carefully choosing the radiation frequency, intensity and polarization, a significant amount of population can be transferred, and this transfer is known as optical pumping.

The simplest forms of optical pumping are illustrated in Figure 1. Figure 1a shows a model two-state atom, with one ground state and one excited state. The laser field induces transitions between the ground and excited states, and spontaneous emission transfers population from the excited state to the ground state. The net result is that, as long as the laser field is present, a significant population of excited state atoms will exist, i.e., the atoms are "optically pumped" into the excited state. If the laser field is turned off, spontaneous emission causes all the atoms to decay eventually to the ground state. Exactly what fraction of the atoms are in the excited state when the laser is on (an experimentally very important number) is determined by the strength of the laser field, its frequency with respect to the atomic resonance, and the transition probability of the atom.

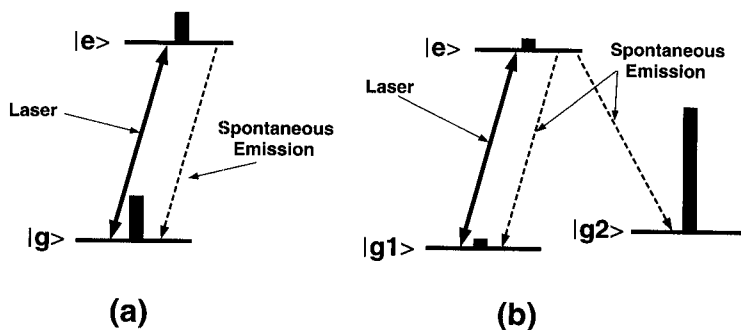


FIG. 1. Building blocks of optical pumping. (a) A two-level atom. The laser, tuned to resonance, stimulates transitions between the ground state $|g\rangle$ and excited state $|e\rangle$, and spontaneous emission transfers population from the excited to the ground state. In the steady state, a population of excited-state atoms is maintained. (b) A three-level atom. The laser stimulates transitions between a first ground state $|g_1\rangle$ and the excited state. Spontaneous emission transfers population back to $|g_1\rangle$, and also to another ground state $|g_2\rangle$. In the steady state, all atomic population will be optically pumped into $|g_2\rangle$.

Figure 1b shows a model three-level atom, in which the laser induces transitions from the ground state to the excited state, and spontaneous emission causes transitions into either of two possible lower states. Atoms can decay back to the original ground state, or they can decay into a new state. If there is no significant transition probability out of the new state, population will continue to accumulate there as long as the laser field is present. Eventually all the atomic population will be transferred to the new state, after which the presence of the laser will have no significant effect.

While Figure 1 illustrates the basic principles of state selection by optical pumping, most atoms have a considerably more complicated level structure than is shown in either Figure 1a or 1b. Generally, an atom will have one or more hyperfine levels in the ground state, each one of these will have degenerate magnetic sublevels, and there will be a variety of states—distinct, degenerate, or quasidegenerate—in the excited-state manifold. Nevertheless, the processes shown in Figure 1 can be thought of as the building blocks of the optical pumping process, and as such they provide a useful framework in which to analyze qualitatively the behavior of a given system.

9.3 Calculations of the Optical Pumping Process

In the process of analyzing the feasibility of an experiment, an important step involves making predictions of such things as signal to noise and total count rate expected. Thus, it is important to be able to estimate the population fraction that

the optical pumping process can produce in the desired atomic state. Unfortunately, a great number of difficult-to-characterize experimental parameters affect the optical pumping process to some degree; also, a number of nuances in the photon-atom interaction, relating to coherence, might affect the outcome. Because of these complications, it is sometimes difficult to make truly accurate predictions of the results of a particular optical pumping setup. Nevertheless, experience has shown that reasonable estimates can be obtained by following a few guidelines.

Leaving discussion of some of the potential complications until later, I begin with a rate equation approach to calculating the optical pumping process. Rate equation calculations are relatively simple and give accurate results in many situations. They are based on the phenomenological Einstein model, in which each state of the atom is assigned a population n_i , and population transfer between the states occurs via stimulated and spontaneous emission.

9.3.1 Two-Level Atoms

Assuming a very narrow band laser tuned exactly to the peak of the atomic resonance, the two-level case of Figure 1a has the rate equations [2]

$$\dot{n}_g = QIn_e - QIn_g + \Gamma n_e, \quad (9.1)$$

$$\dot{n}_e = -QIn_e + QIn_g - \Gamma n_e, \quad (9.2)$$

where n_g and n_e are the ground and excited state populations, respectively, Γ is the transition rate for spontaneous decay, I is the laser intensity (i.e., the energy per unit area per second), and Q is the stimulated rate per unit intensity. The first two terms in Eqs. (9.1) and (9.2) describe stimulated emission into and out of the ground state, and the third term describes spontaneous emission. Note that if Eqs. (9.1) and (9.2) are added, the result is $\dot{n}_{\text{tot}} \equiv \dot{n}_g + \dot{n}_e = 0$, which is as expected, because the total number of atoms does not change.

The coefficient Q is given by

$$Q = \frac{8\pi |\boldsymbol{\varepsilon} \cdot \mathbf{d}|^2}{c\hbar^2 \Delta\omega_0}, \quad (9.3)$$

where c is the speed of light, \hbar is Planck's constant divided by 2π , $\boldsymbol{\varepsilon}$ is the electromagnetic field polarization vector, \mathbf{d} is the dipole matrix element of the atomic transition, and $\Delta\omega_0$ is the full width at half maximum atomic line width (in radians per second). The derivation of Eq. (9.3) involves using time-dependent perturbation theory to obtain the transition rate for an atom in an electromagnetic field, and then averaging over the atomic line shape. It is a little too lengthy to include here, but it is discussed in reference [2].

Equation (9.3) can be simplified in the case of an atom whose line shape is determined entirely by spontaneous emission. In this case, $\Delta\omega_0 = \Gamma$, and use can

be made of the relationship [3] between the magnitude of the dipole matrix element and the spontaneous decay rate Γ , i.e.,

$$d^2 = \frac{3\hbar c^3}{4\omega_0^3} \Gamma, \quad (9.4)$$

where ω_0 is the frequency of the atomic transition (in radians per second). With this simplification,

$$Q = \frac{3\lambda^3}{2\pi ch} |\boldsymbol{\varepsilon} \cdot \hat{\mathbf{d}}|^2, \quad (9.5)$$

where $\lambda = 2\pi c/\omega_0$ is the wavelength of the atomic resonance radiation, and $\hat{\mathbf{d}}$ is the unit vector along the dipole moment \mathbf{d} . The quantity $|\boldsymbol{\varepsilon} \cdot \hat{\mathbf{d}}|^2$ ranges between zero and one and contains dipole selection rule information associated with the transition. It is unity for a truly two-level atom, and hence can be ignored for the present. It will be important, however, in the later discussion of multilevel atoms.

The steady-state value of n_e , obtained by setting the time derivatives to zero in Eqs. (9.1) and (9.2), is

$$n_e = \frac{QI}{2QI + \Gamma} n_{\text{tot}}. \quad (9.6)$$

Note that for $I \rightarrow \infty$, $n_e \rightarrow \frac{1}{2}n_{\text{tot}}$, or at most only half the atoms can be pumped into the excited state. It is common practice to define a saturation intensity I_{sat} such that when $I = I_{\text{sat}}$, one-fourth of the atoms are excited (assuming $|\boldsymbol{\varepsilon} \cdot \hat{\mathbf{d}}|^2 = 1$). Thus,

$$I_{\text{sat}} \equiv \frac{\Gamma}{2Q} = \frac{\pi\hbar c\Gamma}{3\lambda^3}. \quad (9.7)$$

The rate equations then take on the convenient form

$$\dot{n}_g = \frac{I}{2I_{\text{sat}}} \Gamma(n_e - n_g) + \Gamma n_e, \quad (9.8)$$

$$\dot{n}_e = -\frac{I}{2I_{\text{sat}}} \Gamma(n_e - n_g) - \Gamma n_e, \quad (9.9)$$

This form allows straightforward solution of the equations, with the natural lifetime of the transition as the unit of time. To apply Eqs. (9.8) and (9.9) to a given two-level atomic transition, then, all that is needed is the natural transition probability Γ and the wavelength λ . Γ , which is equivalent to the Einstein A coefficient, is tabulated for a number of atomic transitions of interest in Table I; values of Γ for a great many other atomic transitions can be found in reference [4].

9.3.2 Multilevel Atoms

For many situations, extension of the rate equations to multilevel atoms is simply a matter of adding terms to take account of stimulated and spontaneous emission for each additional state. When a complete set of equations is arrived at, the solution can be obtained using standard numerical methods for solving coupled linear differential equations [5].

The type of multilevel problem that is of interest for state preparation of atoms often consists of optical pumping between two or more manifolds of magnetic sublevels. The preferential population of one or more of the magnetic sublevels of a particular state is often the goal of the optical pumping process, because the result is an atomic population that is oriented or aligned in the laboratory. To correctly determine the individual state-to-state stimulated and spontaneous emission rates for this situation, account must be taken of the branching ratios and selection rules for different possible transitions to or from a given level. This information is contained in the quantity $|\mathbf{\epsilon} \cdot \hat{\mathbf{d}}|^2$.

TABLE I. Optical Pumping Parameters for Several Atoms

| Atom | Transition | λ (nm) | $\Gamma/2\pi$ (MHz) ^a | I_{sat} (mW/cm ²) ^b |
|------------------------|--------------------------|----------------|----------------------------------|---|
| Alkalis: | | | | |
| Li | $2S_{1/2}-2P_{1/2, 3/2}$ | 670.8 | 5.8 | 2.5 |
| Na | $3S_{1/2}-3P_{1/2}$ | 589.6 | 10 | 6.4 |
| | $3S_{1/2}-3P_{3/2}$ | 589.0 | 10 | 6.4 |
| K | $4S_{1/2}-4P_{1/2}$ | 769.9 | 6.1 | 1.7 |
| | $4S_{1/2}-4P_{3/2}$ | 766.5 | 6.2 | 1.8 |
| Rb | $5S_{1/2}-5P_{1/2}$ | 794.8 | 5.4 | 1.4 |
| | $5S_{1/2}-5P_{3/2}$ | 780.1 | 5.9 | 1.6 |
| Cs | $6S_{1/2}-6P_{1/2}$ | 894.3 | 4.4 | 0.80 |
| | $6S_{1/2}-6P_{3/2}$ | 852.1 | 5.2 | 1.1 |
| Alkaline earths: | | | | |
| Ca | $4^1S_0-4^1P_1$ | 422.6 | 35 | 61 |
| Ba | $6^1S_0-6^1P_1$ | 553.5 | 19 | 15 |
| Metastable rare gases: | | | | |
| He | $2^3S_1-2^3P_{0,1,2}$ | 1083 | 1.6 | 0.16 |
| Ne | $^3P_2-\alpha_9$ | 640.2 | 6.9 | 3.4 |
| Ar | $^3P_2-\alpha_9$ | 811.5 | 5.9 | 1.4 |
| Other atoms: | | | | |
| Cr | $4^7S_3-4^7P_2^0$ | 429.0 | 5.0 | 8.3 |
| | $4^7S_3-4^7P_3^0$ | 427.5 | 4.9 | 8.2 |
| | $4^7S_3-4^7P_4^0$ | 425.4 | 5.0 | 8.5 |

^a The transition probability Γ is given divided by 2π , as this corresponds to the natural line width in megahertz observed spectroscopically.

^b The saturation intensity I_{sat} is calculated from Eq. (9.7).

For an atom with resolvable hyperfine structure, the complete specification of a magnetic substate consists of the orbital angular momentum L , the spin S , their combination J , the nuclear spin I , the total angular momentum F , and the magnetic quantum number M . For a transition between an "excited" level specified by (L, S, J, I, F, M) and a "ground" level specified by (L', S', J', I', F', M') ,¹ the branching ratio factor is given by [6]

$$|\boldsymbol{\varepsilon} \cdot \hat{\mathbf{d}}|^2 = (2F + 1)(2F' + 1)(2J + 1)(2J' + 1)(2L + 1) \\ \times \begin{Bmatrix} L' & J' & S \\ J & L & 1 \end{Bmatrix}^2 \begin{Bmatrix} J' & F' & I \\ F & J & 1 \end{Bmatrix}^2 \begin{pmatrix} F' & F & 1 \\ M' & -M & q \end{pmatrix}^2, \quad (9.10)$$

where the braces denote a 6- j symbol, the large parentheses denote a 3- j symbol, and q is ± 1 for σ^\pm light or 0 for linearly polarized light [7]. If an atom has no hyperfine structure (i.e., $I = 0$), Eq. (9.10) is still valid; one need only set $I = 0$, $F = J$, and $F' = J'$. As complicated as Eq. (9.10) seems, in many cases the 6- j symbols are the same for all transitions and can be ignored for practical purposes, leaving only the 3- j symbol. The 6- j symbols do need to be considered, however, when several different F -levels (or J -levels) in either the excited or ground state are part of the optical pumping process.

For the stimulated terms, Eq. (9.10) is used in expression (9.5) for the stimulated rate Q . For the spontaneous emission terms, the rate for a specific M to M' transition is given by $\Gamma |\boldsymbol{\varepsilon} \cdot \hat{\mathbf{d}}|^2$. It should be noted that all magnetic sublevels within a given hyperfine level have the same total decay rate Γ ; this rate is "split up" into the possible decay channels according to the values of $|\boldsymbol{\varepsilon} \cdot \hat{\mathbf{d}}|^2$. This is reflected in the fact that all the $|\boldsymbol{\varepsilon} \cdot \hat{\mathbf{d}}|^2$ coefficients for spontaneous decay from a given M -level add to unity, as predicted by the sum rules for 3- j and 6- j coefficients.

As a specific example of how a multilevel problem is set up, consider the optical pumping of sodium on the $3S_{1/2}(F' = 2) \rightarrow 3P_{3/2}(F = 3)$ transition, ignoring any role that might be played by other hyperfine levels in the atom. This transition has many of the elements contained in the optical pumping of almost any atomic transition, and it has seen a wide range of applications. The level structure is shown in Figure 2. The quantum numbers (L', S', J', I', F') are $(0, \frac{1}{2}, \frac{1}{2}, \frac{3}{2}, 2)$ for the $3S_{1/2}(F' = 2)$ ground state and $(L, S, J, I, F) = (1, \frac{1}{2}, \frac{3}{2}, \frac{3}{2}, 3)$ for the $3P_{3/2}(F = 3)$ excited state. The $F' = 2$ state has five magnetic sublevels, corresponding to values of M' ranging from -2 to $+2$, and the $F = 3$ excited state has seven sublevels, corresponding to $M = -3 \dots +3$. Altogether, then, there are 12 state populations to follow.

In the absence of a magnetic field, all the magnetic sublevels in each hyperfine state are degenerate. Which transitions are induced by the laser, however,

¹ I follow the convention of labeling ground-state levels with primes, and excited-state levels without primes.

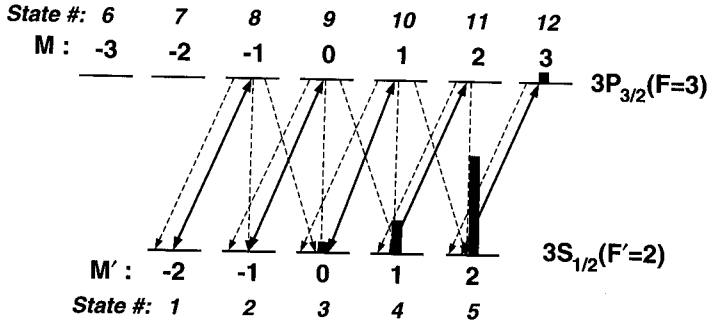


FIG. 2. Optical pumping of the $3S_{1/2}(F' = 2) \rightarrow 3P_{3/2}(F = 3)$ transition in sodium with circularly polarized light. Selection rules limit laser-stimulated transitions to $\Delta M = +1$ for σ^+ light, and spontaneous emission transfers population with $\Delta M = 0, \pm 1$. The result is a transfer of population to the $M' = +2$ state, which corresponds to a spin-polarized (both electronic and nuclear) ground state, and the $M = +3$ state, which consists of a spin-polarized, orbitally oriented state. The state numbers refer to the numbering scheme in Eqs. (9.11)–(9.20).

depends on optical selection rules and the polarization of the laser. For instance, if σ^+ (or σ^-) circularly polarized laser light is used, only transitions with $\Delta M = +1$ (or -1) are allowed. If linearly polarized light is used, only $\Delta M = 0$ is allowed. Thus, the number and character of the equations is different, depending on the polarization of the light.

The case of circularly polarized light is of specific interest because it has been used to create populations of spin-polarized ground-state, and also pure angular momentum, spin-polarized excited-state, sodium atoms [8]. For σ^+ (i.e., left-handed circularly polarized) light [9], transitions to the excited states $|3, -3\rangle$ and $|3, -2\rangle$ are never stimulated, so these states can be eliminated from the rate equations (here the notation $|F, M\rangle$ is used to denote a given magnetic state, with $L, S, J,$ and I dropped for simplicity). Ten equations then describe the remaining states, taking into account stimulated transitions between $|2', -2'\rangle$ and $|3, -1\rangle$; $|2', -1'\rangle$ and $|3, 0\rangle$; etc., as well as all the possible spontaneous transitions. For compactness in the equations, the states can be numbered 1 to 12, starting with $|2', -2'\rangle$ and moving from left to right across the ground and then the excited state, as shown in Figure 2. The 10 equations for σ^+ optical pumping are then

$$\dot{n}_1 = \frac{I}{2I_{\text{sat}}} \frac{\Gamma}{15} (n_8 - n_1) + \frac{\Gamma}{15} n_8, \quad (9.11)$$

$$\dot{n}_2 = \frac{I}{2I_{\text{sat}}} \frac{\Gamma}{5} (n_9 - n_2) + \frac{8\Gamma}{15} n_8 + \frac{\Gamma}{5} n_9, \quad (9.12)$$

$$\dot{n}_3 = \frac{I}{2I_{\text{sat}}} \frac{2\Gamma}{5} (n_{10} - n_3) + \frac{2\Gamma}{5} n_8 + \frac{3\Gamma}{5} n_9 + \frac{2\Gamma}{5} n_{10}, \quad (9.13)$$

$$\dot{n}_4 = \frac{I}{2I_{\text{sat}}} \frac{2\Gamma}{3} (n_{11} - n_4) + \frac{\Gamma}{5} n_9 + \frac{8\Gamma}{15} n_{10} + \frac{2\Gamma}{3} n_{11}, \quad (9.14)$$

$$\dot{n}_5 = \frac{I}{2I_{\text{sat}}} \Gamma (n_{12} - n_5) + \frac{\Gamma}{15} n_{10} + \frac{\Gamma}{3} n_{11} + \Gamma n_{10}, \quad (9.15)$$

$$\dot{n}_8 = \frac{I}{2I_{\text{sat}}} \frac{\Gamma}{15} (n_1 - n_8) - \Gamma n_8, \quad (9.16)$$

$$\dot{n}_9 = \frac{I}{2I_{\text{sat}}} \frac{\Gamma}{5} (n_2 - n_9) - \Gamma n_9, \quad (9.17)$$

$$\dot{n}_{10} = \frac{I}{2I_{\text{sat}}} \frac{2\Gamma}{5} (n_3 - n_{10}) - \Gamma n_{10}, \quad (9.18)$$

$$\dot{n}_{11} = \frac{I}{2I_{\text{sat}}} \frac{2\Gamma}{3} (n_4 - n_{11}) - \Gamma n_{11}, \quad (9.19)$$

$$\dot{n}_{12} = \frac{I}{2I_{\text{sat}}} \Gamma (n_1 - n_8) - \Gamma n_{12}. \quad (9.20)$$

Given the symmetry of the magnetic sublevels, the equations for σ^- optical pumping are identical to Eqs. (9.11)–(9.20) with a simple relabeling of states. The equations for linear polarized excitation will of course be different, but similar in character.

Before solving Eqs. (9.11)–(9.20) numerically, it is useful to observe a few qualitative features. For instance, as always should be the case, $\dot{n}_{\text{tot}} \equiv \sum_i \dot{n}_i = 0$ (this provides a useful check to make sure the coefficients are correct!). Furthermore, the evolution of the population can be followed by inspection, with the help of Figure 2. It should be clear that as time progresses, population will be transferred to states with more and more positive values of M , eventually leading to a steady-state configuration that is reduced to a two-level system with population in only the $|2', 2'\rangle$ and $|3, 3\rangle$ states. This is, in fact, one of the main reasons why optical pumping of this transition in sodium has seen so much application. On one hand, the generation of a two-level atom allows experimental

tests of a number of fundamental quantum electrodynamical phenomena. On the other hand, sodium in the $|2', 2'\rangle$ ground state is a completely spin-polarized atom, with nuclear and electron spin both oriented in the laboratory. The orientation, either parallel or antiparallel to the propagation direction of the laser light, can be selected by pumping with either σ^+ or σ^- light. Similarly, the state $|3, 3\rangle$ is a state with electron spin, nuclear spin, *and* orbital angular momentum oriented in the laboratory.

Using the rate equations, the analysis of circularly polarized excitation in sodium can then be broken down into (a) determining the time it takes to reach the two-level condition (the optical pumping time), which is found by solving the time-dependent rate equations, and (b) determining the steady-state excited $|3, 3\rangle$ population fraction, which can be obtained using Eq. (9.6) for a two-level system. A similar analysis can be applied to linear polarized excitation, but the steady-state excited state population is found by solving the simultaneous equations obtained when all time derivatives are set to zero.

When we compare linear to circularly polarized excitation, an important point must not be overlooked. When the selection rule $\Delta M = 0$ is invoked for linearly polarized excitation, an assumption is made that the axis of quantization is *along the electric vector of the laser field*. The selection rule $\Delta M = \pm 1$ for circularly polarized light, on the other hand, assumes the quantization axis to be *along the direction of light propagation*. Thus, care must be exercised when interpreting the results of an optical pumping calculation in the reference frame of the laboratory.

9.3.3 Laser Frequency Dependence and Power Broadening

Until now, all the rate equations that have been discussed assume an infinitely narrow laser frequency tuned exactly to the center of the atomic resonance. It is possible, under some circumstances, to extend the applicability of rate equations to situations in which the laser frequency is still narrow, but detuned from the center of the atomic resonance by an amount Δ . As will be discussed in more detail later, this is possible when there are no other nearby atomic levels, and when the long-time behavior (compared to $1/\Gamma$) is of interest.

While a correct treatment requires the optical Bloch equations, the dependence on Δ can be introduced into the rate equation approach by arguing that the instantaneous stimulated rate QI is dependent on Δ because the atomic transition has an instantaneous Lorentzian line shape with a full width at half maximum of Γ . This argument is borne out by comparison with exact optical Bloch equation results [2]. Thus, an extra factor

$$\mathcal{L} = \frac{\Gamma^2}{\Gamma^2 + 4\Delta^2} \quad (9.21)$$

is included in all the stimulated rate terms. This can be done for a two-level atom, and also for a multilevel atom such as the one shown in Figure 2, where there are only two energies involved.

With the addition of Δ -dependence, the two-level steady-state excited-state population [Eq. (9.6)] becomes

$$n_c = \frac{QI\mathcal{L}}{2QI\mathcal{L} + \Gamma} n_{\text{tot}} \quad (9.22)$$

$$= \frac{\Gamma^2(I/I_{\text{sat}})}{2[\Gamma^2 + 4\Delta^2 + \Gamma^2(I/I_{\text{sat}})]} n_{\text{tot}}. \quad (9.23)$$

It is evident from examination of Eq. (9.23) that with increasing intensity, the profile broadens because the center of the line saturates earlier than the wings. The full width at half maximum $\delta\omega_{\text{FWHM}}$ of the power broadened profile described by Eq. (9.23) is given by

$$\delta\omega_{\text{FWHM}} = \Gamma[1 + (I/I_{\text{sat}})]^{1/2}. \quad (9.24)$$

It should be emphasized that Eq. (9.23) describes the *steady-state* frequency dependence of the excited-state population. Because of the intensity dependence in Eq. (9.23), it is tempting to say that the atomic transition is power-broadened. It must be remembered, however, that this is only true in the steady state; the instantaneous (i.e., on a time scale short compared to the stimulated rate) atomic line width is still governed by the unbroadened line shape given in Eq. (9.21).

Power broadening is a very real effect in most practical situations, since saturation intensities are generally a few milliwatts per square centimeter, and a laser with diameter of order 1 mm and power only a few milliwatts can have an intensity of several hundred milliwatts per square centimeter. Thus, the line width observed in a laser-induced fluorescence measurement of a beam of atoms will almost always be power-broadened unless that laser intensity is kept to a minimum.

9.3.4 Limitations of Rate Equations

While rate equations provide a practical tool for evaluating a broad range of optical pumping systems, it must be remembered that they represent only an approximate solution. If they are to be used in a given situation, some understanding of what is left out is essential in order to avoid misleading results. In this section an attempt is made to set out some guidelines for the appropriate use of rate equations. The assumption is that in many instances they will still provide a

useful tool for evaluating experiments in state selection, even though in some cases they clearly are inadequate.

The major omission in a rate equation approach is any coherences that might develop between the quantum states of the system. In a fully quantum treatment of a system of atomic levels, the full state of the system is described by a set of complex amplitudes, one for each atomic level in the system. If one allows for a number of possible sets of amplitudes, each with a given probability, the system is properly described by a density matrix. In general, there will be specific phase relationships between the complex amplitudes for each level, and these relative phases represent coherences between the states. The relative phases show up as off-diagonal elements in the density matrix. Since rate equations follow state populations, which are associated with the square magnitudes of the complex amplitudes, or just the diagonal elements of the density matrix, they do not keep track of the relative phases, and hence have no coherence information.

Exact treatment of the coherence between levels in a two-level system can be obtained using the optical Bloch equations. In a multilevel system, such as might be encountered in a state-selection experiment, extensions of the optical Bloch equations can be used, though the problem rapidly becomes a complex one. Discussion of the optical Bloch equations is beyond the scope of this work; for such a discussion and some approaches to the multilevel problem, the reader is encouraged to consult references [2, 10, 11]. Instead, let us concentrate on the following question: Given a specific set of atomic levels and a laser to pump them, will a rate equation approach be adequate for predicting what we want to know about the system? To answer this, the following queries should be useful.

9.3.4.1 Are Transient Populations Important? If the experiment to be carried out relies only on steady-state populations produced by cw (or quasi-cw) laser illumination, rate equations may well be quite adequate. If not, there may be problems. For example, a major, well-known effect that is not seen in a rate equation treatment is Rabi oscillations. These are a manifestation of coherence induced by the laser between the ground and excited states, and consist of transient oscillations in the atomic population between the ground and excited state. Their frequency (given by $\omega_R = \Gamma(I/2I_{\text{sat}})^{1/2}$ for a two-level atom [2]) is determined by the stimulated rate, and they can cause as much as a 100% movement in population between the ground and the excited states. They do decay, however, on the time scale of the natural lifetime (or faster in the presence of collisions), and when they have decayed, the state populations often follow the rate equation predictions quite closely. So, if the state distribution of the atom within the first natural lifetime or two after the laser is turned on is important, rate equations should not be used.

It should be noted that in some situations it is not completely trivial to determine if the experiment to be performed is sensitive to transient populations,

since the eventual population distribution in the steady state could depend on transient effects. This occurs, for example, in the case of circularly polarized excitation of sodium when one considers the influence of the other hyperfine levels $F' = 1$ and $F = 2$. The $F' = 1$ state lies 1772 MHz below the $F' = 2$ state, and the $F = 2$ state lies 59.6 MHz below the $F = 3$ state. Before the population is completely transferred to the $|2', 2'\rangle \rightarrow |3, 3\rangle$ system, where it is isolated by selection rules from all other atomic levels, there is some probability that the $F = 2$ state will be excited, because it is only a few atomic line widths away from the $F = 3$ state. This opens the pathway for decay into the $F' = 1$ ground state during the transient period before optical pumping is complete. Thus, how many atoms find their way into the $|2', 2'\rangle \rightarrow |3, 3\rangle$ two-level system depends critically on the transient behavior of the state populations, the correct modeling of which requires more than rate equations.

9.3.4.2 Do Coherences Matter for the Planned Experiment? Even in the steady state, coherences are induced between all states connected by the laser. These coherences do not appear in a rate equation approach, so if the experiment is somehow sensitive to them, rate equations should not be used. In some cases, the effect of these coherences can be dramatic. For instance, if two different ground-state sublevels are coupled by two lasers to the same excited state, it can happen that there is no steady-state excited state population. This phenomenon, known as coherent population trapping [12], is a result of the coherence that develops between the two ground-state sublevels. It does not show up in a rate equation treatment of this situation. In some situations, however, it can be put to use if population transfer between two ground states is desired without subjecting the atoms to spontaneous emission [13].

One must take care, however, not to be misled by trivial coherences induced by coordinate rotations. Consider, for example, linearly polarized excitation of a $J' = 0 \rightarrow J = 1$ transition. With a quantization axis along the electric vector of the linearly polarized light, the selection rule $\Delta M = 0$ applies, and the system becomes a simple two-level atom. The rate equation approach will work just fine. If one insists, however, on a quantization axis along the direction of the light propagation, then the linearly polarized light must be broken down into σ^+ and σ^- components, which are coherent with each other. The result is a coherent excitation of the $|1, 1\rangle$ and the $|1, -1\rangle$ states. The coherence between these two states, which must be maintained to get the right answer, will be lost in a rate equation approach. Thus, before applying the rate equations, it is important to rotate the coordinate system of a given problem to a system that eliminates as many coherences as possible.

In sum, it can be said that rate equations can be used in situations where the steady-state populations are of interest, and where coherence either does not matter or cannot develop between more than two states (ground and excited) at a time. As a result, a simple situation such as that shown in Figure 2 is quite

appropriate for rate equations. However, cases with multiple excited levels within a few natural line widths, or multiple lasers tuned to the same state, should be approached with caution.

9.4 Calculations and Experimental Reality

Even if the rate equation approach were exact for all situations, its usefulness (and, indeed, the usefulness of any theory) can still be hampered by a number of experimental factors that can influence the outcome of an optical pumping setup. These factors must be taken into account in planning an experiment, and an evaluation made as to whether they will have a significant influence. If the effect of these factors is unknown or ignored, it is useless to perform any modeling calculations because the predicted results could be dramatically different from reality. The following discussion covers a number of effects that can influence the optical pumping process.

9.4.1 Laser Spatial Profile

In a crossed-beam arrangement, where the laser beam intersects the atom beam at 90° , the laser spatial profile has two effects. The profile along the direction of motion of atoms translates into a time-dependent laser intensity for the atoms, because the atoms are travelling with some velocity v . This can be taken into account relatively easily by using a time-dependent intensity in the rate equations. It must be remembered, however, that (a) not all atoms travel with the same velocity, so some averaging will need to be done over the velocity distribution of the atoms, and (b) if the time dependent intensity varies too rapidly, there may be important nonadiabatic or transient effects. The profile transverse to the atom beam is important because if it is nonuniform, different parts of the atom beam experience different laser intensities. If the optical pumping process is strongly intensity dependent, a nonuniformly pumped atom beam will result.

9.4.2 Doppler Shift Effects

Because of the relatively high velocity of thermal atoms, and the precision with which a laser is tuned to the atomic frequency in an optical pumping experiment, the Doppler shift can be a substantial effect. If an atom is traveling at exactly 90° to the laser beam, there will be no first-order Doppler shift. However, atom beams and laser beams generally have some amount of divergence, so there will always be a range of angles between the atomic trajectories and the laser. The result is that atoms in different parts of the beam will experience different laser frequencies, shifted by an amount

$$\delta\omega = \mathbf{k} \cdot \mathbf{v} = \omega \frac{v}{c} \cos \theta, \quad (9.25)$$

where \mathbf{k} is the wave vector of the laser light, \mathbf{v} is the velocity of the atom, $\omega = 2\pi c/\lambda$ is the laser frequency, and θ is the angle between \mathbf{k} and \mathbf{v} . As an example, consider a thermal sodium beam pumped on the 589 nm resonance line. For $\theta = 1$ degree (17 mrad), $\delta\nu \equiv \delta\omega/2\pi = 24$ MHz, a quite significant shift compared to the natural line width of 10 MHz. Of course, not only do different parts of the beam experience different laser frequencies, but there is also the thermal velocity spread in the beam, which results in a range of Doppler shifts for any given position in the beam. Clearly, the Doppler shifts in a given experiment must be estimated and either deemed insignificant or averaged over before optical pumping calculations can be relied on.

9.4.3 Atom Deflection Effects

In addition to ordinary Doppler shifts, there can arise more complicated effects resulting from the deflection of the atom beam by light pressure. Because the optical pumping process usually involves a number of spontaneous emission events, there will in general be a net transfer of momentum from the laser to the atom. Thus, as the atom passes through the optical pumping region, the atom is accelerated along the laser propagation direction, resulting in a changing Doppler shift as a function of time. The transverse acceleration of the beam depends on the laser intensity, the detuning, and the instantaneous Doppler shift; it is given by [14]

$$\mathbf{a} = \frac{\Gamma \hbar \mathbf{k}}{2m} \frac{I/I_{\text{sat}}}{1 + I/I_{\text{sat}} + 4[(\Delta - \mathbf{k} \cdot \mathbf{v})/\Gamma]^2}. \quad (9.26)$$

For sodium with $I \gg I_{\text{sat}}$, \mathbf{a} can be as large as 10^6 m/s², which means that the angle that the atom beam makes with respect to the laser direction changes by about 1 mrad per millimeter of travel along the beam. Under some circumstances, the changing Doppler shifts induced by this changing angle have significant effects on the optical pumping process.

9.4.4 Incomplete Laser Polarization

In the ideal optical pumping experiment, the polarization of the laser is assumed to be exactly as specified—100% circularly polarized, for example. Because of imperfect polarizers, natural birefringence in windows, and reflection effects which occur in a real experimental situation, this is often not the case. It is thus important to make an estimate of how sensitive an optical pumping scheme is to the “wrong” polarization. Often, the effects are not severe if the amount of “wrong” polarization is small. In a circularly polarized $J \rightarrow J + 1$

optical pumping scheme such as the one in Figure 2, the effect is only a somewhat incomplete transfer of the population to the desired sublevels. The effects, if small, can be estimated with rate equations, but one should be aware of the possible coherences between excited sublevels that would be neglected.

Situations with more levels must be treated with more care, however. The case of sodium is an example of this. The problem arises from the loss mechanism to $F' = 1$ mentioned earlier under transient effects. If the polarization of the pumping laser is not completely circular, the loss mechanism is no longer transient. With imperfect σ^+ light, there is always some probability that the $|2', 2'\rangle$ state will make a transition to the $|3, 1\rangle$, or worse, the $|2, 1\rangle$ state, from which the pathway is open to the $F' = 1$ state. Because of the nature of rate equations, if a pathway to a population "sink" exists, the only true steady-state solution consists of all population eventually in the "sink." Thus, a laser with only slightly impure polarization can result in a total loss of population from the desired steady-state result.

9.4.5 Magnetic Fields

Magnetic fields can have profound effects on the optical pumping process in the situation where one is trying to produce a specific distribution of magnetic sublevels in the atoms. First of all, magnetic fields will Zeeman-shift the energy levels, changing the effective frequency of the laser. For an atom with hyperfine structure in a field that is not too strong, this shift is given by [15]

$$\Delta\omega_Z = \frac{eB}{2m_e} g_F M, \quad (9.27)$$

where B is the magnetic field strength in teslas, m_e is the electron mass, M is the magnetic quantum number, and

$$g_F = g_J \frac{F(F+1) + J(J+1) - I(I+1)}{2F(F+1)}, \quad (9.28)$$

with

$$g_J = 1 + \frac{J(J+1) + S(S+1) - L(L+1)}{2J(J+1)}. \quad (9.29)$$

If the atom does not have hyperfine structure, Eq. (9.27) still holds, with F replaced by J . For example, the Zeeman shift of the $|3, 3\rangle$ sublevel of the $3P_{3/2}$ level in sodium is $\Delta\omega_Z/2\pi = 2.8 \times 10^4$ MHz/tesla.

More troublesome, however, is the fact that the atomic angular momentum will precess if there is a magnetic field that is not along the quantization axis. This precession is related to the Zeeman effect, and the rotation of the atomic angular momentum vector (in radians per second) is given by the same expression (9.27), multiplied by $\sin \alpha$, where α is the angle between the quantization

axis and the magnetic field. The result is that the orientation of the atom, or equivalently, the magnetic sublevel population distribution, will change with time. In the case of the sodium $|2', 2'\rangle$ state in a field perpendicular to the original quantization axis, the orientation changes at 8.9×10^{10} radians per second per tesla. At a thermal velocity of 800 m/s, this corresponds to a rotation of 6 degrees after traveling only 1 cm in a 10^{-7} tesla (1 milligauss) field.

Besides ruining the atomic orientation, this precession also has an effect similar to incomplete polarization in any situation analogous to circularly polarized pumping of sodium. Because the precession causes a continual redistribution of population toward sublevels with smaller M , the opportunity to make transitions to the $F = 2$ sublevels is always there. Again, this opens the loss channel to $F' = 1$, making the complete loss of population a possibility.

From a practical point of view, then, magnetic fields must be well controlled in an optical pumping experiment. Ideally, they should be reduced to the 10^{-7} tesla (1 milligauss) level to prevent unwanted precession and Zeeman shifts. In some circumstances, however, a weak "guide" field (i.e., weak enough to cause minimal Zeeman shifts but strong enough to overpower any residual stray fields) can be applied along the desired quantization axis, provided other aspects of the experiment are not sensitive to this field.

9.4.6 Radiation Trapping

This effect can lead to problems in experiments where high-density atomic beams are employed [16]. If the density is high enough, the fluorescence emitted by an optically pumped atom can be large enough to affect the optical pumping of neighboring atoms. Since this fluorescence comes from arbitrary directions and has varying polarization, the result is a redistribution of magnetic sublevel populations. As a rule of thumb, atomic densities below about 10^{10} atoms-cm $^{-3}$ are generally safe from radiation trapping. A check can be made relatively simply by carrying out the experiment to be done with the optically pumped atoms at a range of atomic densities and observing whether the outcome varies. Theoretical calculations can also be made based on numerical simulations if so desired [17].

9.5 Diagnosis of an Optically Pumped Beam

While calculations provide a very useful guide for setting up an experiment, the possible theoretical shortcomings and experimental pitfalls are such that some sort of probe of the state distribution should be carried out before an experimental result can be relied on. Usually some sort of spectroscopic probe can be arranged, especially since there will generally be laser light available from the optical pumping.

Diagnosis of experiments that involve degenerate magnetic sublevel populations, such as alignment or orientation of an alkali atom, have been approached by a number of methods. A very straightforward method is to expose the atoms to a magnetic field strong enough to Zeeman-shift the magnetic sublevels to the point where they are resolvable spectroscopically. The relative populations can then be observed by monitoring the relative peak heights in a laser-induced fluorescence spectrum. This method has been used with sodium [18, 19] and appears to work quite well. Care must be exercised on a few points, however. The method could prove problematic if the experiment to be done with the optically pumped atoms is sensitive to magnetic fields. In principle, it is possible to arrange for the experiment to be conducted in a field-free region, after which the atoms enter the magnetic field, but one must always worry about how well isolated the experimental region is. Furthermore, changes can occur in the magnetic sublevel population on entering the magnetic field if it is not along the quantization axis defined for the optical pumping, or if there are strong field gradients.

Another approach involves measuring the degree of polarization and angular dependence of the fluorescence in either the optical pumping region itself or in a probe region. This method has the advantage that no magnetic fields need to be applied, but has the disadvantage of sometimes relying on some degree of modeling of the state distribution.

When a given population distribution in an excited-state magnetic sublevel manifold decays and emits fluorescence, the light intensity and polarization will have well-defined angular dependencies. Each excited magnetic sublevel contributes to the intensity according to the decay paths open to it, as dictated by the selection rules $\Delta M = 0, \pm 1$. The contribution from each decay path is determined by the relevant Clebsch–Gordan coefficient. The angular dependence of the intensity is given by $\sin^2 \theta$ for $\Delta M = 0$ transitions, or $(1 + \cos^2 \theta)/2$ for $\Delta M = \pm 1$, where θ is the angle between the quantization axis (\hat{z}) and the direction of observation. The polarization of the light for $\Delta M = 0$ transitions is linear along \hat{z} for $\theta = \pi/2$. For $\Delta M = \pm 1$, the light propagating along $\theta = 0$ is circular, σ^\pm , but the light propagating along $\theta = \pi/2$ is linear in the plane perpendicular to \hat{z} [20].

To probe an excited state, then, the fluorescence from the optical pumping region can be analyzed and used to infer the relative sublevel populations. In some cases it may be desirable to characterize the sublevel population distribution in terms of state multipoles. These can provide a physical picture of the excited-state configuration, which may lead to some insights. Reference [16] provides more details on this technique as applied to sodium.

A ground-state distribution can be investigated by using a very weak probe of well-characterized polarization. Using knowledge of the selection rules and Clebsch–Gordan coefficients, it is possible to predict what excited-state magnetic

sublevel populations would be produced by the probe, given a specific ground state distribution, assuming no saturation or optical pumping.² The polarization and angular distribution of the probe fluorescence can then be predicted, and measurements compared with this. This approach is not a direct measurement, since it relies on first modeling the ground state population, and then seeing if the model agrees with experiment, but nevertheless it can be used with success in many instances [21].

In cases where fluorescence probes are not convenient and the ground-state magnetic sublevel population distribution is of interest, another approach, making use of a Stern–Gerlach-type magnetic field, can be utilized [22]. The atom beam is passed through a region of magnetic field \mathbf{B} with a strong gradient, and the spatial profile is measured downstream. The atoms feel a deflection force $\mathbf{F} = (\boldsymbol{\mu} \cdot \nabla)\mathbf{B}$ according to their magnetic moment $\boldsymbol{\mu}$, which is related to their magnetic quantum number M by $\boldsymbol{\mu} = \mu_B g_F M \hat{z}$ [μ_B is the Bohr magneton $e\hbar/2m_e$, and g_F is the g -factor, given by Eq. (9.28)]. With a suitable arrangement of strong fields and long flight times, individual peaks corresponding to each magnetic sublevel can be resolved in the spatial profile of the atom beam. The relative populations can then be easily monitored as a function of optical pumping parameters. Of course, as in the case with Zeeman separation of the sublevels, one must be extremely careful with stray magnetic fields when using this technique.

9.6 Specific Atoms

This chapter ends with a discussion of some experimental aspects of specific atomic species that have been or could be optically pumped for a state-selected experiment. The atoms are grouped in categories that have similar properties, with a few general words about each category. Tables I and II contain relevant parameters for the transitions of interest in the species discussed. For atoms not discussed here, energy levels can be found in reference [23], transition probabilities can be found in reference [4], some hyperfine structure information is available in reference [24], and some isotope shifts can be found in reference [25].

9.6.1 Alkalis

The combination of a simple electronic structure, strong resonance transitions in the visible or near infrared, and relative ease of forming an atomic beam has made alkali atoms a popular choice for many applications.

²Optical pumping and even saturation can begin to occur at very low power levels. The experimenter is warned to resist the temptation to turn up the power to get a little more signal in this type of experiment!

For state-selected collision studies, as well as other applications, sodium has been widely used [8, 19, 21, 26–32]. A good description of the fundamentals of sodium optical pumping, as applied to state selection, has been given by Hertel and Stoll [26]. Atomic beams can be formed with oven temperatures in the 300–400°C range, and the strong D_1 and D_2 lines, at 589.6 and 589.0 nm respectively, lie within the peak range of the laser dye rhodamine 6G. There is only one stable isotope, ^{23}Na , which has a nuclear spin $I = 3/2$. Thus, the atom has hyperfine structure, and it generally must be resolved in an optical state-preparation experiment. Laser line widths of order 1 MHz are required for

TABLE II. Hyperfine Splittings (HFS) for Selected Isotopes^a

| Isotope | Abundance | I | State | HFS [F -splitting (MHz)- F] ^b |
|-------------------|-----------|-------|------------|---|
| ^6Li | 7.4% | 1 | $2S_{1/2}$ | $\frac{1}{2}-228-\frac{3}{2}$ |
| | | | $2P_{1/2}$ | $\frac{1}{2}-26.2-\frac{3}{2}$ |
| | | | $2P_{3/2}$ | $\frac{5}{2}-3.2-\frac{3}{2}-1.9-\frac{1}{2}$ |
| ^7Li | 92.6% | $3/2$ | $2S_{1/2}$ | 1-803.5-2 |
| | | | $2P_{1/2}$ | 1-92-2 |
| | | | $2P_{3/2}$ | 3-9.3-2-5.9-1-2.8-0 |
| ^{23}Na | 100% | $3/2$ | $3S_{1/2}$ | 1-1772-2 |
| | | | $3P_{1/2}$ | 1-189-2 |
| | | | $3P_{3/2}$ | 0-16.5-1-35.5-2-59.6-3 |
| ^{39}K | 94% | $3/2$ | $4S_{1/2}$ | 1-462-2 |
| | | | $4P_{1/2}$ | 1-56-2 |
| | | | $4P_{3/2}$ | 0-3.3-1-9.4-2-21-3 |
| ^{85}Rb | 72.2% | $5/2$ | $5S_{1/2}$ | 2-3035.7-3 |
| | | | $5P_{1/2}$ | 2-362.1-3 |
| | | | $5P_{3/2}$ | 1-29.3-2-63.4-3-120.7-4 |
| ^{87}Rb | 27.8% | $3/2$ | $5S_{1/2}$ | 1-6834.7-2 |
| | | | $5P_{1/2}$ | 1-812-2 |
| | | | $5P_{3/2}$ | 0-72.3-1-157.1-2-267.2-3 |
| ^{133}Cs | 100% | $7/2$ | $6S_{1/2}$ | 3-9192.6-4 |
| | | | $6P_{1/2}$ | 3-1168-4 |
| | | | $6P_{3/2}$ | 2-151-3-201-4-251-5 |
| ^{53}Cr | 9.6% | $3/2$ | 7S_3 | $\frac{3}{2}-206.5-\frac{5}{2}-289.1-\frac{7}{2}-371.7-\frac{9}{2}$ |
| | | | 7P_2 | $\frac{1}{2}-40-\frac{3}{2}-66-\frac{5}{2}-93-\frac{7}{2}$ |
| | | | 7P_3 | $\frac{9}{2}-7-\frac{7}{2}-5-\frac{5}{2}-4-\frac{3}{2}$ |
| | | | 7P_4 | $\frac{11}{2}-65-\frac{9}{2}-53-\frac{7}{2}-41-\frac{5}{2}$ |

^a It should be noted that in an atomic beam consisting of a mixed isotopic sample, the hyperfine manifolds of the isotopes will generally be offset from each other by the isotope shift.

^b F -values are displayed with the lowest energy level first.

this, so a frequency-stabilized cw dye laser, pumped by a visible argon ion laser, is necessary.

One aspect of single-frequency optical pumping in sodium that must be kept in mind is the potential for transfer between hyperfine ground states [10]. In some cases this may be the desired optical pumping process, but in others the goal may be to maintain a closed system in which the atoms interact repeatedly with the laser photons. Transfer to the other hyperfine level represents loss to the experiment in this case. While it is possible in principle to tune only to the $F' = 2 \rightarrow F = 3$ transition in the D_2 line, so that transitions to $F' = 1$ are forbidden by the $\Delta F = 0, \pm 1$ selection rule, in practice the $F = 3$ state is not perfectly resolved from the $F = 2$ state, being separated by only 59.6 MHz. The $F' = 2 \rightarrow F = 2$ transition has a wing which overlaps the $F' = 2 \rightarrow F = 3$ frequency, and this wing can be quite significant, especially if there is power broadening.

An experimental solution to this problem has been to perform the optical pumping with two laser frequencies, separated by 1712 MHz. One laser frequency is tuned to the $F' = 2 \rightarrow F = 3$ transition, and the other is tuned to the $F' = 1 \rightarrow F = 2$ transition, returning atoms that may have been optically pumped into the wrong state. The extra laser frequency can be generated with either an electro-optic or acousto-optic modulator. Electro-optic modulators produce the second laser frequency without spatial separation, and they always make a symmetric pair of sideband frequencies at plus and minus the modulation frequency. This can be put to advantage by modulating at 856 MHz (an easier frequency to work with) and utilizing the two side bands instead of the carrier frequency. Electro-optic modulators tend to be somewhat inefficient, however, so many experimenters have used acousto-optic modulators. These spatially separate the shifted beam, and they only shift in one direction at a time, the direction being chosen by the angle of incidence on the modulator.

The optical pumping of cesium has also been extensively studied, mainly because of its application in atomic clocks [33], and also because the D_2 line at 852.1 nm falls within the range of inexpensive diode lasers [34]. The only stable isotope, ^{133}Cs , has nuclear spin $7/2$. The hyperfine splitting is much larger than in sodium, so the problem of loss to the "wrong" ground-state hyperfine level is less important. Nevertheless, optical pumping with two laser frequencies is often advantageous, because more of the atomic population can be accessed. To achieve this, two or more diode lasers can be used (they are, after all, quite inexpensive), or the frequency of the laser can be modulated by varying the injection current [35].

Rubidium has also been the subject of a number of optical pumping studies, a great majority of which have been in a vapor cell. The D_1 and D_2 lines, at 794.8 and 780.0 nm, respectively, are also accessible to diode lasers, so it is a good candidate for an inexpensive experiment. There are two stable isotopes, ^{85}Rb

(72.2% abundance, $I = 5/2$) and ^{87}Rb (27.8% abundance, $I = 7/2$), each of which has well-resolved hyperfine structure. The two isotopes with significant natural abundance make rubidium unsuitable for an experiment in which all the atoms in the beam must be identically state-selected, such as some collision experiments (though it is in principle possible to use more lasers and pump all atoms). Rubidium has, however, seen wide application in experiments where the existence of other isotopes does not interfere with the measurements, such as in the field of cooling and trapping [36].

Lithium, with its two stable isotopes ^6Li and ^7Li , has also been optically pumped [37], though it poses some special problems. The laser wavelength required is 670.8 nm for both the D_1 and D_2 lines, which are separated by 10 GHz. This wavelength can be accessed with a single-frequency stabilized dye laser operating with DCM laser dye, or with a visible laser diode. The problems arise because the hyperfine structure is not well resolved, especially in ^7Li . To avoid the loss mechanism to the “wrong” hyperfine ground state, as discussed for sodium, two-frequency optical pumping is a necessity. For state-selection of ground state atoms, this is not a problem, but if a significant population of excited states is desired, one must be aware of the possibility of coherent population trapping. Coherently exciting the same excited state from two ground-state hyperfine levels could greatly reduce excited-state populations [12]. A possible way to circumvent some of these problems is to use isotopically enriched ^6Li , though this can increase the cost of the experiment.

Potassium, with D -lines at 769.9 and 766.5 nm, has seen little use as an optical pumping target for state-selective experiments. The wavelengths require a Ti:sapphire laser, or a dye laser with LDS700 laser dye and a krypton ion pump laser. In principle, however, there is no reason why it could not be optically pumped in the same way as the other alkali atoms.

9.6.2 Alkaline Earths

While not as popular as the alkalis, some alkaline earths have been optically pumped to provide state-selected targets. The attraction of these atoms lies in the simple 1S_0 ground state and 1P excited states. The excited P -state can be aligned and/or oriented, and collisions can be studied without the complication of spin polarization.

Barium can be optically pumped on the $6^1S_0 \rightarrow 6^1P_1$ transition (wavelength 553.5 nm) using rhodamine 110 laser dye [38]. There are quite a few naturally occurring isotopes of barium (134, 135, 136, 137, 138), but these are well separated spectroscopically, so they do not pose a significant problem unless the whole atom beam must be state-selected. A possible cause for caution in using barium is the metastable 6^1D_2 level, to which the 6^1P_1 level can decay. The branching ratio for the 6^1P_1 going to the ground state vs. the 6^1D_2 state is 425 : 1.

This ratio is fairly large, so if the optical pumping process is modeled with rate equations and monitored experimentally (to the extent possible), the loss mechanism can be kept under control.

Calcium has a similar line, the $4^1S_0 \rightarrow 4^1P_1$ transition at 422.6 nm, which can be optically pumped with a dye laser using stilbene 3 laser dye pumped by a UV argon ion laser [39]. An alternative source of radiation for this wavelength is a Ti:sapphire laser doubled in an external buildup cavity [40]. Isotope shifts and hyperfine structure are not a problem for calcium, because it is naturally 97% ^{40}Ca , which has zero nuclear spin. As with barium, there is an intermediate metastable 4^1D state, to which population can decay from the excited state. In this case, though, the branching ratio is $10^5:1$ in favor of the ground state, so population loss can almost always be ignored.

9.6.3 Metastable Rare Gas Atoms

While excitation of rare gas atoms from the ground state to the lowest-lying excited states generally requires many electron volts of energy (i.e., VUV photons), they all have metastable states, easily generated in discharge sources, which can be optically pumped in the near infrared. Applications have included state-selected collision studies, polarized electron sources, and cooling and trapping.

Helium has seen wide application in state-selected experiments, both as a collision participant [41] and as a source of polarized electrons [42]. The 2^3S_1 metastable state (19.8 eV above the ground state) has accessible transitions to the $2^3P_{0,1,2}$ states at 1.083 μm wavelength. This wavelength can be generated with a specially adapted Ti:sapphire laser, pumped by a visible argon ion laser [43], with a laser using a LNA crystal as its gain medium [44], or with recently available laser diodes.

Metastable neon has also been optically pumped [45–48]. The two metastable states are 3P_2 and 3P_0 , at 16.6 and 16.7 eV above the ground state, respectively. These levels can be excited to an array of states of the configuration $1s^22s^22p^53p$, denoted in the Paschen notation by $\alpha_1 \cdots \alpha_{10}$. Of all these excited states, only the α_9 state [$2p^5(^2P_{1/2})3p, J = 3$] can be excited without opening the possibility of cascade down to the ground state and subsequent loss of population. The wavelength for the transition to this from 3P_2 is 640.2 nm, accessible with DCM laser dye. Like the $^3S_1 \rightarrow ^3P_2$ transition in helium, this transition has the right sublevel configuration ($J \rightarrow J + 1$) to allow creation of a spin-polarized, oriented target, as may be desirable for state-selected collision experiments. The natural isotope distribution of neon is 91% ^{20}Ne and 9% ^{22}Ne . Both of these have zero nuclear spin, so there is no hyperfine structure. There is an isotope shift, however, so the ^{22}Ne line is separated from the ^{20}Ne line by 1630 MHz.

Argon is similar to neon. The 3P_2 and 3P_0 states are metastable, with energies of 11.5 and 11.7 eV above the ground state, respectively. The transition most useful for optical pumping is from the 3P_2 state to the $3p^5(^2P_{3/2})4p(J=3)$, or α_9 state, with wavelength 811.5 nm [49]. This wavelength is obtainable with a dye laser, a Ti:sapphire laser, or a diode laser. Naturally occurring argon is 99.6% ^{40}Ar , with zero nuclear spin, so hyperfine splitting and isotope shifts are not important in this case.

9.6.4 Other Atoms

Besides the alkalis, the alkaline earths, and the metastable rare gases, few other atoms have been optically state-selected in an atomic beam. Chromium has been optically pumped to produce a polarized high-spin target for collision studies with polarized electrons [50]. The $^7S_3 \rightarrow ^7P_4^0$ transition at 425.43 nm is accessible with a dye laser operating with stilbene 3 laser dye pumped by a UV argon ion laser. The natural isotope abundance contains 84% ^{52}Cr , 4% ^{50}Cr , and 2% ^{54}Cr , all of which have no hyperfine structure, and 10% ^{53}Cr , which has hyperfine structure with $I = 3/2$. The ^{50}Cr 425.43 nm line has an isotope shift of about 132 MHz relative to the ^{52}Cr line; the ^{54}Cr isotope shift is negligible, however.

References

1. Happer, W. (1972). *Rev. Mod. Phys.* **44**, 169.
2. Allen, L., and Eberly, J. H. (1987). *Optical Resonance and Two-Level Atoms*. Dover, New York.
3. See, e.g., Woodgate, G. K. (1970). *Elementary Atomic Structure*, Chapter 3. McGraw-Hill, London.
4. Wiese, W. L., Smith, M. W., and Glennon, B. M. (1966). "Atomic Transition Probabilities—Hydrogen through Neon," Vol. I, *NSRDS-NBS* **4**; Wiese, W. L., Smith, M. W., and Miles, B. M. (1969). "Atomic Transition Probabilities—Sodium through Calcium," Vol. II, *NSRDS-NBS* **22**; Martin, G. A., Fuhr, J. R., and Wiese, W. L. (1988). "Atomic Transition Probabilities—Scandium through Manganese," *J. Phys. Chem. Ref. Data* **17**, Suppl. 3; Fuhr, J. R., Martin, G. A., and Wiese, W. L. (1988). "Atomic Transition Probabilities—Iron through Nickel," *J. Phys. Chem. Ref. Data* **17**, Suppl. 4.
5. See, e.g., Press, W. H., Flannery, B. P., Teukolsky, S. A., and Vetterling, W. T. (1986). *Numerical Recipes*. Cambridge University Press, Cambridge.
6. See, e.g., Edmonds, A. R. (1960). *Angular Momentum in Quantum Mechanics*. Princeton University Press, Princeton.
7. The 3-*j* and 6-*j* symbols are tabulated in a number of places, such as Rotenberg, M. (1959). *The 3-*j* and 6-*j* Symbols*. Technology Press, Cambridge. Alternatively, they are now available in many symbolic manipulation computation packages.
8. McClelland, J. J., Kelley, M. H., and Celotta, R. J. (1989). *Phys. Rev. A* **40**, 2321.

9. The subject of the handedness of circular polarization can be the cause of a significant amount of confusion, though it is discussed in detail in most textbooks on optics. A good explanation can be found in Crawford, F. S., Jr. (1968). *Waves*, p. 400. McGraw-Hill, New York.
10. McClelland, J. J., and Kelley, M. H. (1985). *Phys. Rev. A* **31**, 3704.
11. Farrel, P. M., MacGillivray, W. R., and Standage, M. C. (1988). *Phys. Rev. A* **37**, 4240.
12. Gray, H. R., Whitley, R. M., and Stroud, C. R., Jr. (1978). *Opt. Lett.* **3**, 218.
13. Bergmann, K. (1991). In *Atomic Physics 12*, J. C. Zorn and R. R. Lewis (eds.), p. 336. American Institute of Physics, New York.
14. See, e.g., Lett, P. D., Phillips, W. D., Rolston, S. L., Tanner, C. E., Watts, R. N., and Westbrook, C. I. (1989). *J. Opt. Soc. Am. B* **6**, 2084.
15. See, e.g., Woodgate, G. K. (1970). *Elementary Atomic Structure*, pp. 183ff. McGraw-Hill, London.
16. Fischer, A., and Hertel, I. V. (1982). *Z. Phys. A* **304**, 103.
17. Kunasz, C. V., and Kunasz, P. B. (1975). *Comp. Phys. Comm.* **10**, 304.
18. Cusma, J. T., and Anderson, L. W. (1983). *Phys. Rev. A* **28**, 1195.
19. Han, X. L., Schinn, G. W., and Gallagher, A. (1988). *Phys. Rev. A* **38**, 535.
20. See, e.g., Jackson, J. D. (1975). *Classical Electrodynamics*, 2nd Edition, Section 9.2. J. Wiley & Sons, New York.
21. Lorentz, S. R., Scholten, R. E., McClelland, J. J., Kelley, M. H., and Celotta, R. J. (1993). *Phys. Rev. A* **47**, 3000.
22. Riddle, T. W., Oneillian, M., Dunning, F. B., and Walters, G. K. (1981). *Rev. Sci. Instrum.* **52**, 797.
23. Moore, C. E. (1971). *Atomic Energy Levels*, Vols. I and II, *NSRDS-NBS* **35**.
24. Radzig, A. A., and Smirnov, B. M. (1985). *Reference Data on Atoms, Molecules and Ions*, pp. 99ff. Springer Verlag, Berlin.
25. King, W. H. (1984). *Isotope Shifts in Atomic Spectra*. Plenum, New York.
26. Hertel, I. V., and Stoll, W. (1978). *Adv. At. Mol. Phys.* **13**, 113.
27. Balykin, V. I. (1980). *Opt. Comm.* **33**, 31.
28. Jaduszliwer, B., Dang, R., Weiss, P., and Bederson, B. (1980). *Phys. Rev. A* **21**, 808.
29. Dreves, W., Kamke, W., Broermann, W., and Fick, D. (1981). *Z. Phys. A* **303**, 203.
30. Hils, D., Jitschin, W., and Kleinpoppen, H. (1981). *Appl. Phys.* **25**, 39.
31. Scholten, R. E., Shen, G. F., and Teubner, P. J. O. (1993). *J. Phys. B* **26**, 987.
32. Sang, R. T., Farrell, P. M., Madison, D. H., MacGillivray, W. R., and Standage, M. C. (1994). *J. Phys. B* **27**, 2711.
33. Vanier, J., and Audoin, C. (1989). *Quantum Physics of Atomic Frequency Standards*. Adam Hilger, Bristol.
34. Wieman, C. E., and Holberg, L. (1991). *Rev. Sci. Instrum.* **62**, 1.
35. Watts, R. N., and Wieman, C. E. (1986). *Opt. Comm.* **57**, 45.
36. See, e.g., Sheehy, B., Shang, S.-Q., Watts, R., Hatamian, S., and Metcalf, H. (1989). *J. Opt. Soc. B* **6**, 2165.
37. Baum, G., Caldwell, C. D., and Schröder, W. (1980). *Appl. Phys.* **21**, 121.
38. Register, D. F., Trajmar, S., Csanak, G., Jensen, S. W., Fineman, M. A., and Poe, R. T. (1983). *Phys. Rev. A* **28**, 151; Zetner, P. W., Trajmar, S., Csanak, G., and Clark, R. F. H. (1989). *Phys. Rev. A* **39**, 6022.
39. Law, M. R., and Teubner, P. J. O. (1993). In *Abstracts of Contributed Papers to the XVIII ICPEAC*, p. 150, T. Andersen, B. Fastrup, F. Folkman, and H. Knudsen (eds.). Aarhus, Denmark.

40. Polzik, E. S., and Kimble, H. J. (1991). *Opt. Lett.* **16**, 1400.
41. Hart, M. W., Hammond, M. S., Dunning, F. B., and Walters, G. K. (1989). *Phys. Rev. B* **39**, 5488.
42. Rutherford, G. H., Ratliff, J. M., Lynn, J. G., Dunning, F. B., and Walters, G. K. (1990). *Rev. Sci. Instrum.* **61**, 1490.
43. Oro, D. M., Lin, Q., Soletsky, P. A., Zhang, X., Dunning, F. B., and Walters, G. K. (1992). *Rev. Sci. Instrum.* **63**, 3519.
44. Schearer, L. D., Leduc, M., Vivien, D., Lejus, A.-M., and Thery, J. (1986). *IEEE J. Quant. Elec.* **QE22**, 713; Lynn, J. G., and Dunning, F. B. (1986). *Rev. Sci. Instrum.* **61**, 1996.
45. Gaily, T. D., Coggiola, M. J., Peterson, J. R., and Gillen, K. T. (1980). *Rev. Sci. Instrum.* **51**, 1168.
46. Hotop, H., Lorenzen, T., and Zartrow, A. (1981). *J. Electr. Spect. and Rel. Phenom.* **23**, 347.
47. Bussert, W. (1986). *Z. Phys. D* **1**, 321.
48. Brand, J. A., Furst, J. E., Gay, T. J., and Schearer, L. D. (1992). *Rev. Sci. Instrum.* **63**, 163.
49. Giberson, K. W., Hammond, M. S., Hart, M. W., Lynn, J. G., and Dunning, F. B. (1985). *Opt. Lett.* **10**, 119.
50. Hanne, G. F., McClelland, J. J., Scholten, R. E., and Celotta, R. J. (1993). *J. Phys. B* **29**, L753.